

# COMPLEX WAVELET TRANSFORM BASED HYPER ANALYTICAL IMAGE DENOISING BY BIVARIATE SHRINKAGE TECHNIQUE

S.Sasi Pavan Kumar<sup>1</sup> , Dr.T.Sreenivasulu Reddy<sup>2</sup>

<sup>1</sup>(Pg Scholar, Dept Of Electronics & Communication Engineering, SVU Engineering College, Tirupati)

<sup>2</sup>(Professor, Dept Of Electronics & Communication Engineering, SVU Engineering College, Tirupati)

**Abstract**—Removal of noise is an important step in the image restoration process, but de-noising of image remains a challenging problem in recent research associated with image processing.

De-noising is used to remove the noise from corrupted image, while retaining the edges and other detailed features as much as possible. This noise gets introduced during acquisition, transmission, reception, storage and retrieval processes. Here we retrieve de-noised image using Bivariate Shrinkage Technique. Out of many wavelet transforms here Discrete Wavelet Transform, Dual Tree Wavelet Transform and Hyper Analytical Wavelet transforms are implemented on different noisy images. Here the noisy image is assumed to be complex image and its real part and imaginary parts are separated. These are subjected to Bi-shrink filter separately into different stages of decomposition depending upon the severity of noise. The obtained de-noise image is compared with original image using different parametric measures like Peak Signal to Noise Ratio, Structural similarity Index measure, Covariance and Root mean square Error whose values are tabulated. The values of retrieved image obtained yields much better visual effect and hence this method is said to be a better one when compared with de-noising methods using Weiner Filter and various Local Adaptive Filters.

## I. INTRODUCTION

Digital images play an important role both in daily life applications such as satellite television, computed tomography as well as in areas of research and technology such as geographical information systems and astronomy. In reality, an image is mixed with certain amount of noise which decreases visual quality of image[1][9]. Therefore, removal of noise in an image is a very common problem in recent research fields of image processing. An image gets corrupted with noise during acquisition or at transmission due to channel errors or errors in storage media due to faulty hardware[1][2]. Removing noise from the noisy image is

still a challenging problem for researchers. Noise may be classified as substitutive noise (impulsive noise: e.g., salt and pepper noise, random valued impulse noise etc.) additive noise (e.g., additive white Gaussian noise) and multiplicative noise (e.g. speckle noise). However, here the investigation has been limited to additive white Gaussian noise[1]. In general, the goal of any noise removal scheme is to suppress noise as well as to preserve details and edges of image as much as possible. Removal of noise is an important aspect in the image processing.

Figure. 1 shows the basic model for de-noising of image. In the implementation of these methods, first the noisy image is decomposed by wavelet transform. After this, by using Bivariate shrinkage technique the decomposed images are subjected to de-noising process where the output is given to Shrink Thresholding. Finally de-noised image is obtained by using inverse wavelet transform as shown in figure 1.

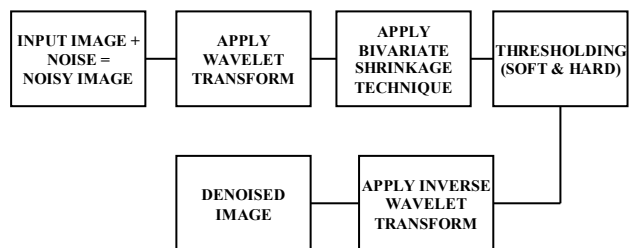


**Figure: 1** Image de-noising Process using Bivariate Shrinkage Technique

Consider an image is corrupted with additive Gaussian white noise. The noisy image can be modelled as:

$$y(i, j) = x(i, j) + n(i, j) \quad (1)$$

Where  $y(i, j)$  is the noisy image,

$x(i, j)$  is the original image and

$n(i, j)$  is additive Gaussian white noise.

The goal of image de-noising is to suppress noise from noisy image with minimum mean square error. Here, the wiener filter minimizes the mean square error between the estimated image  $\hat{x}(i, j)$  and the original image  $x(i, j)$ [1][7]. This error measure can be expressed as:

$$e^2 = E[(x(i, j) - \hat{x}(i, j))^2] \quad (2)$$

Wiener filter is used to measure an image pixel by pixel and compares the neighbourhoods of size M-by-N to estimate the local image mean and standard deviation[1][7]. Here it assumes that the noise is stationary with zero mean and variance  $\sigma_n^2$  and uncorrelated with the original image  $x(i, j)$ . Based on these assumptions wiener filter estimates local mean and variance around each pixel using (3) and (4) as below:

$$\mu = \frac{1}{MN} \sum_{i,j \in k} y(i, j) \quad (3)$$

$$\sigma^2 = \frac{1}{MN} \sum_{i,j \in k} y^2(i, j) - \mu^2 \quad (4)$$

Where  $\mu$  is local mean and  $\sigma^2$  is local variance.

Then wiener filter creates a pixel wise filtering using these estimates and the estimated image is given in (5) as below:

$$\hat{x}(i, j) = \mu + \frac{\sigma^2 + \sigma_n^2}{\sigma^2} (y(i, j) - \mu) \quad (5)$$

Where  $\sigma_n^2$  is noise variance, if noise variance is not given, wiener filter uses average of all local estimated variances.

The Wiener filter in the wavelet domain removes the noise pretty well in the smooth regions but performs poorly along the edges. That is why it performs better on smooth images like Lena than on images with edges like the cameraman. For a noise variance of 400, the MSE was found to be 107.5 for the cameraman image and 80.5 for the Lena image.

In Global Wiener filtering, the above expression for a Wiener filter is applied over the whole image. This method does a good job at de-blurring; however, it behaves very poorly in the presence of large noise[2][3]. The Wiener filter would work well for an image which has similar local statistics throughout the entire image. However in most natural images, the first order statistics vary from one part of an image to another and hence its poor performance in the presence of large noise. The advantage of this method is that it is not computationally intensive and works well for smooth images[1][4].

When Wiener filtering is performed on small blocks of an image at a time, the method is called Local Wiener Filtering. In this method, the PSD (Power Spectral Density) of the unregarded image is estimated for each block[4]. This calculated PSD is then used in the expression of the Wiener filter. Thus, the local statistics are also accounted for in the calculation of the Wiener filtered image[6]. Images with many edges are handled much better by the local Wiener filter than the global Wiener filter. We used a window of size of  $3 \times 3$  in the calculation of the local Wiener filtered image. The drawback of this method is that it is more computationally demanding[6][1].

The de-noising of the image is done in the following procedural steps. First select an image, check whether it is grey image or colour Image. If it is a colour

image then firstly convert this image into grey image. Then use it as input image[1][4].

- The image is further decomposed into four stages approximation, horizontal, vertical and diagonal versions. The horizontal, vertical and diagonal steps of the image are called details of the image.
- The approximation step is further processed for decomposition. The approximation is further carried out and divided into four steps again for three decompositions.
- The decomposed images are retrieved by comparing approximation coefficients and details coefficients. This process is carried out by preceding the decomposition levels. The coefficients obtained in first stage are considered as finally obtained ones.
- The retrieved coefficients are then succeeded for soft thresholding and subjected to Inverse wavelet Transform.

Here we have considered Dual tree and Hyper Analytical wavelet transforms where the give image is considered as complex one and is sub divided into real and imaginary parts. The marginal variance of the coefficients of the image is calculated separately for both real and imaginary images[5].

- Finally, calculate PSNR between original image and noisy image and PSNR between the de-noised image and original image.

## PROPOSED WORK

### BIVARIATE SHRINKAGE FILTER

Bivariate shrinkage model undergoes the following calculations. There are strong dependencies between neighbour coefficients such as between a coefficient, its parent (adjacent coarser scale locations), and their siblings (adjacent spatial locations).

Let  $w_2$  represents the parent of  $w_1$  ( $w_2$  is the wavelet coefficient at the same position as  $w_1$ , but at the next coarser scale.) Then

$$y_1 = w_1 + n_1$$

$$y_2 = w_2 + n_2$$

Where  $y_1$  and  $y_2$  are noisy observations of  $w_1$  and  $w_2$ ,

$n_1$  and  $n_2$  are noise samples. We can write

$$y = w + n$$

where  $w=(w_1, w_2)$ ,  $y = (y_1, y_2)$  and  $n = (n_1, n_2)$

The estimator for  $w$  given the corrupted observation  $y$  is

$$W_s = \text{arg} \max_{W_s} (P_{W_x/W_s}(W_x/W_s))$$

After some manipulations, this equation can be written as

$$\text{arg} \max_{W_s} (P_{W_s/W_x}(W_s/W_x)) \quad (i)$$

$$\text{arg} \max_{W_s} (P_n(W_s - W_x) \cdot P_{W_s}(W_s))$$

For construction of Bi-shrink filter,

Let us assume Gaussian noise is added to the given image then,

$$p_{w_n}(W_n) = \frac{1}{2\pi\sigma_{W_n}^2} e^{-\frac{(W_n^1)^2 + (W_n^2)^2}{2\sigma_{W_n}^2}}$$

For a noise free image it is characterised as,

$$p_{w_s}(W_s) = \frac{3}{2\pi\sigma_{W_s}^2} e^{-\frac{\sqrt{3}}{\sigma_{W_s}} \sqrt{(w_s^1)^2 + (w_s^2)^2}}$$

By substituting the above equation in equation (i) we finally contain the relationship between input and output of the given images,

$$\widehat{W}_s^1 = \frac{\sqrt{(w_x^1)^2 + (w_x^2)^2} - \frac{\sqrt{3}\sigma_{W_n}}{\sigma_{W_s}}}{\sqrt{(w_x^1)^2 + (w_x^2)^2}} \cdot W_x^1$$

Where

$$\sigma_{W_n}^2 = \frac{\text{median}|W_x|}{0.6745}$$

$$\sigma_{W_s} = \frac{\sigma_{W_s^1} + 0.5\sigma_{W_s^2}}{2}$$

**COMPLEX WAVELET TRANSFORMS:**

The complex wavelet transform [11] is divided into different sub transforms among them the following methods are applied for denoising process.

**A. DISCRETE WAVELET TRANSFORMS:**

The DWT transform, to which we will refer to as classical DWT, presented in section is the most commonly used as it is fast, non-redundant and assures the perfect reconstruction. Despite all these properties, classical DWT might not be good enough for some specific applications. In the following, we will present some transforms, derived from DWT, that can be encountered in practical applications.

DWT is largely used for one-dimensional discrete signals. If we want apply the discrete wavelet transform to two-dimensional signals (images, for instance), we need to use the DWT’s extension to two dimensions, namely the 2D DWT.

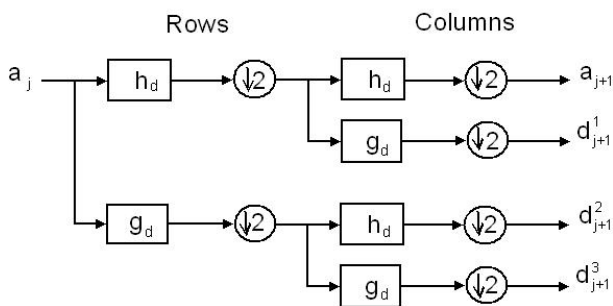


Figure.2 :One-level 2D DWT decomposition scheme

LL (a)	HL (d <sup>2</sup> )
LH (d <sup>1</sup> )	HH (d <sup>3</sup> )

Figure.3 :2D DWT coefficients image

**B. DUAL TREE COMPLEX WAVELET TRANSFORM:**

Kingsbury first introduced the DTCWT, that relies on the observation that approximate shift invariance can be achieved with a real DWT by doubling the sampling rate at each level of the tree. For this to work, the samples must be evenly spaced. The sampling rates can be doubled by eliminating the down-sampling by two after the level one filters. This is equivalent to having two parallel fully-decimated trees a and b, like in below given figure 4. It is found that, to get uniform intervals between samples from the two trees below level one, the filters in one tree must provide delays that are half a sample different (at each filter input rate) from those in the other tree. This statement is also supported by Selesnick who gives an alternative derivation and explanation of the same result.

The implementation of such a transform is done using two mother wavelets, one for each tree, one of them being (approximately) the Hilbert transform of the other. On one hand, the dual-tree DWT can be viewed as an over complete wavelet transform with a redundancy factor of two. On the other hand, the dual-tree DWT is also a complex DWT, where the first and second DWTs represent the real and imaginary parts of a single complex DWT[1][2][5].

Extension of the DT CWT to two dimensions is achieved by separable filtering along columns and then rows. However, if column and row filters both suppress negative frequencies, then only the first quadrant of the 2-D signal spectrum is retained. It is well known, from 2-D Fourier transform theory, that two adjacent quadrants of the spectrum are required to represent fully a real 2-D signal[1][7]. Therefore in the DT CWT it is also filtered with complex conjugates of the row (or column) filters in order to retain a second (or fourth) quadrant of the spectrum. This then gives 4:1 redundancy in the transformed 2-D signal. This below shown figure 4 & 5 defines the 4 trees T = A, B, C and D. If a and b denote approximation and detail coefficients.

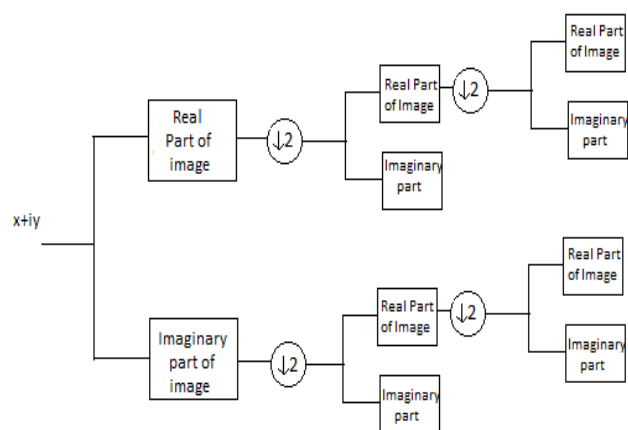


Figure.4 :Analysis part of Dual Tree

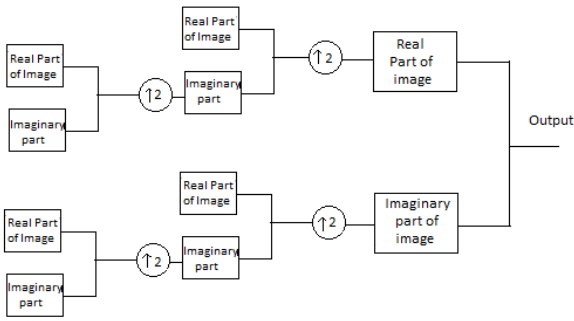


Figure.5 : Synthesis part of Dual tree

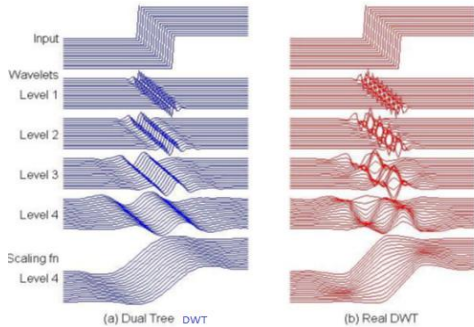


Figure.6: Approximation components at levels 1 to 4 of 16 shifted step responses of the (a) DT CWT and (b) Real DWT

C. [HYPER ANALYTICAL WAVELET TRANSFORM:

In the following we see that the definition of the analytic signal associated to a 2D real signal named hyper complex signal[3][5].

So, the hyper complex mother wavelet associated to the real mother wavelet,  $(x, y)$  is defined as:

$$\varphi_a(x,y) = \varphi(x,y) + iH_x\{\varphi(x,y)\} + jH_y\{\varphi(x,y)\} + kH_x\{H_y\{\varphi(x,y)\}\}$$

where  $i^2 = j^2 = -k^2 = -1$ ,  $ij = ji = k$ ,  $jk = kj = -i$ ,  $ki = ik = -j$  and  $ijk = 1$ ,

The HWT of an image  $f(x,y)$  is:  $\langle f(x,y), \varphi_a(x,y) \rangle$   
 $HWT f\{x,y\} = \langle f(x,y), \varphi_a(x,y) \rangle$

We can conclude that the HWT of the image  $f(x,y)$  can be computed with the aid of the 2D DWT of its associated hyper complex image. In consequence the HWT implementation uses four trees, each one implementing a 2D DWT, thus having a redundancy of four[5]. The first tree is applied to the input image. The second and the third trees are applied to 1D Hilbert transforms computed across the lines ( $H_x$ ) or columns ( $H_y$ ) of the input image. The fourth tree is applied to the result obtained [after the computation of the two 1D Hilbert transforms of the input image][10][5].

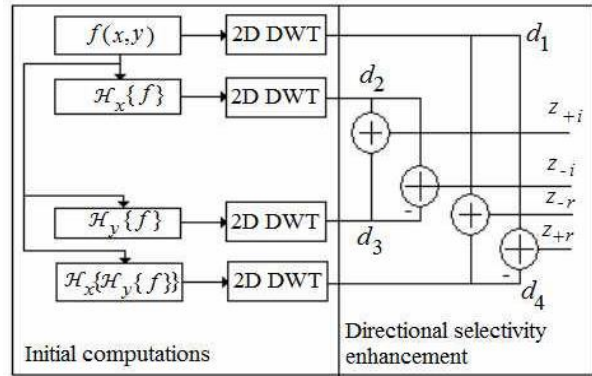


Figure.7 : HWT implementation scheme

The below show figure 8 shows the comparison between DWT, DT CWT, HWT whose input is as shown in below figure.

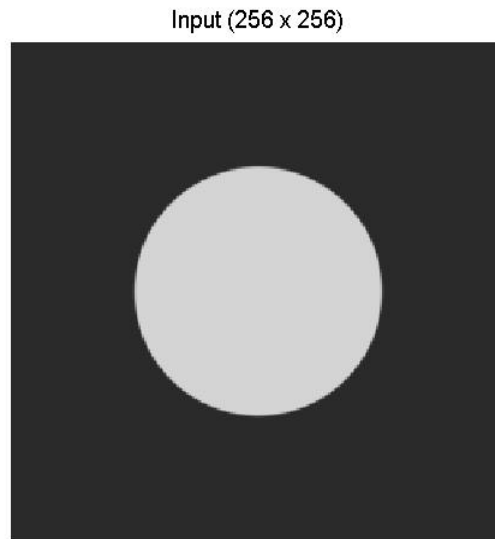


Figure.8 : The 2D image given as input

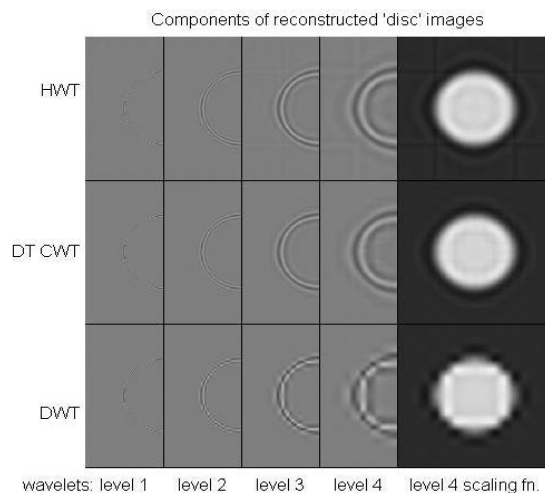


Figure.9 : Outputs of different wavelet transform

Finally, to improve the signal to noise ratio of image by local adaptive wavelet image de-noising method following steps follows: First we apply wavelet transform (DWT) i.e.bior4.4 wavelet to decompose the noisy image into four sub images: LL, HL, LH and HH.

- The next step will be to construct bi-shrink method using several 1-D windows on the direction information contained in each sub image.
- After this apply bi-shrink filter for LL sub image and thresholding to remaining sub images.
- Then reconstructs image by wavelet inverse transform and we get the de-noised image.
- Finally, to calculate PSNR between original image and noisy image and PSNR between the de-noised image and original image.

By seeing the below figure 10 we can conclude that bivariate shrinkage technique when applied sub images could suppress additive Gaussian white noise and preserve the edge of image. There by the results obtained are comparatively far better as of the results obtained by using adaptive Weiner filter.



Figure.10 : 1-D window structures: from left to right: a) 1-D windows for LH, b) 1-D windows for HL and c) 1-D windows for HH.

The image Lena is decomposed using three different wavelet transform techniques as Discrete wavelet Transform, Dual Tree Wavelet Transform and Hyper Analytical Wavelet Transform. The comparison between noisy image and original image is shown in each method. Furthermore the noise image (at noise range of 0.01 to 0.1) when given as input to wiener filter produces a de-noised image and similarly when the noisy image is given as input to bishrink filter gives de-noised image which is visually far better comparatively[1][2].

### III. RESULTS:

#### DUAL TREE WAVELET TRANSFORM:

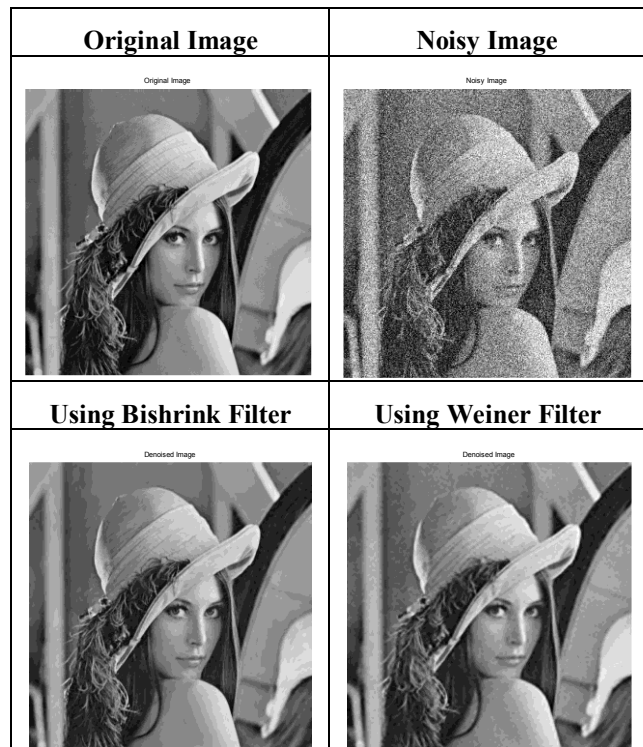


Figure.11: Image de-noising in DT CWT using both Wiener and Bishrink Filters

#### DISCRETE WAVELET TRANSFORM:

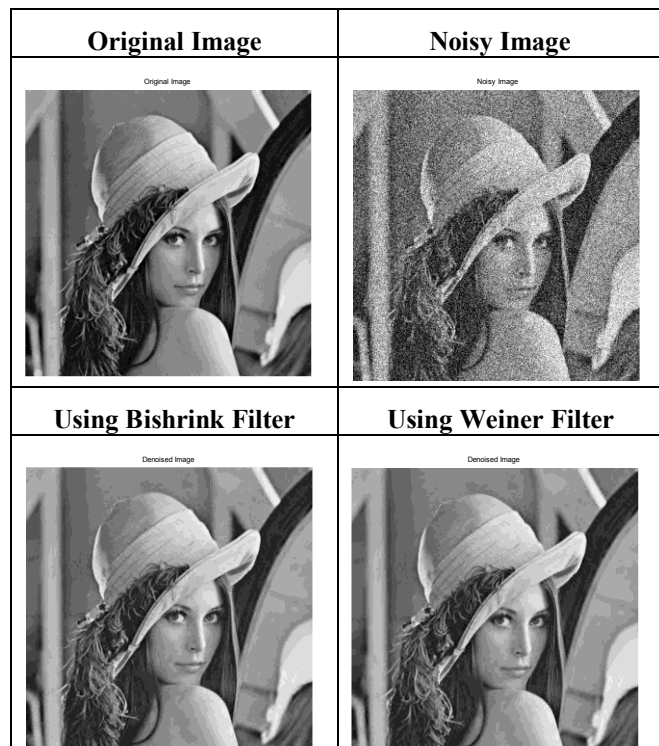
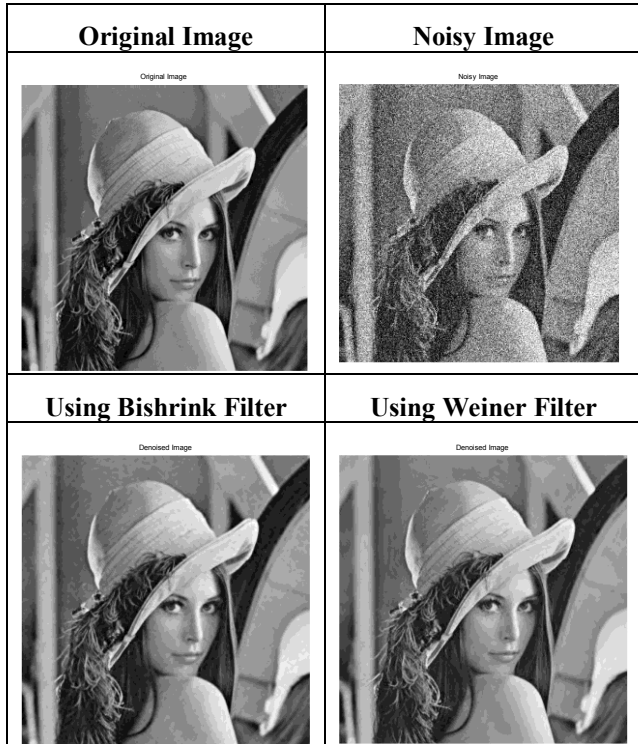


Figure.12: Image de-noising in DWT using both Wiener and Bishrink Filters

**HYPER ANALYTICAL WAVELET TRANSFORM**



**Figure.13:** Image de-noising in HWT using both Wiener and Bishrink Filters

**PEAK SIGNAL TO NOISE RATIO**

$$PSNR = 20 \log_{10} (\max_1) - 10 \log_{10} (MSE)$$

Where

$$MSE = \frac{1}{mn} \sum_{i=0}^{m-1} \sum_{j=0}^{n-1} [i(i, j) - k(i, j)]^2$$

Here  $\max_1$  is maximum possible pixel value of the image

**ROOT MEAN SQUARE ERROR**

$$RMSE = \sqrt{MSE(\hat{\theta})}$$

Where  $(\hat{\theta})$  is estimated which is defined as square root of mean square error

**STRUCTURAL SIMILARITY INDEX MEASURE**

SSIM = Sum of total number of pixels /total number of pixels present in the image.

It measures similarity between the original image and retrieved image.

**CORRELATION COEFFICIENT:**

Correlation Coefficient is used to verify and determine how strongly the recovered image is matched with the original Image.

$$r = \frac{n(\sum xy) - (\sum x)(\sum y)}{\sqrt{[n\sum x^2 - (\sum x)^2][n\sum y^2 - (\sum y)^2]}}$$

Where n is number of pairs of pixels,  $\sum xy$  is sum of product of pixels,  $\sum x$  is sum of x pixels,  $\sum y$  is sum of y pixels.

**Table 1: SSIM Values of each column corresponds to the noise values from (0.01, 0.02 .... 0.1)**

0.2000	0.1390	0.1083	0.0904	0.0791	0.0693	0.0626	0.0583	0.0538	0.0498
0.3823	0.3160	0.2720	0.2441	0.2230	0.2082	0.1971	0.1877	0.1758	0.1684
0.4479	0.3983	0.3521	0.3246	0.3052	0.2857	0.2818	0.2680	0.2546	0.2439
0.4254	0.3659	0.3193	0.2935	0.2747	0.2571	0.2434	0.2353	0.2234	0.2142
0.4910	0.4446	0.4048	0.3793	0.3647	0.3419	0.3315	0.3198	0.3061	0.2969
0.4424	0.3740	0.3242	0.2963	0.2755	0.2567	0.2413	0.2331	0.2213	0.2116
0.4866	0.4370	0.3910	0.3655	0.3445	0.3241	0.3095	0.2984	0.2867	0.2742

**Table 2: RMSE Values of each column corresponds to the noise values from (0.01, 0.02 .... 0.1)**

25.3372	35.1849	42.4954	48.2149	52.9785	57.2227	60.7445	63.7719	66.5456	69.1627
9.9283	12.7274	15.0084	16.8412	18.3772	19.7751	21.0784	22.1745	23.1486	24.1961
7.9943	9.4536	10.8879	11.7979	12.6683	13.6359	14.1504	14.8171	15.5992	16.4111
9.0276	10.9438	12.6359	14.0337	15.1270	16.4107	17.3227	18.3241	19.0992	20.1232
6.9579	8.2314	9.4099	10.2635	10.9204	11.8818	12.4633	13.1657	13.8805	14.6462
8.2661	10.3292	12.0872	13.3964	14.5422	15.7219	16.6162	17.5109	18.3202	19.2562
7.1750	8.5765	9.8701	10.8048	11.5014	12.5426	13.1495	13.8499	14.6117	15.4312

**Table 3: CC Values of each column corresponds to the noise values from (0.01, 0.02 .... 0.1)**

0.8830	0.8015	0.7373	0.6863	0.6451	0.6071	0.5782	0.5522	0.5277	0.5044
0.9784	0.9646	0.9506	0.9374	0.9251	0.9127	0.9005	0.8893	0.8784	0.8662
0.9859	0.9803	0.9740	0.9700	0.9659	0.9612	0.9591	0.9564	0.9527	0.9492
0.9821	0.9736	0.9646	0.9561	0.9488	0.9394	0.9322	0.9238	0.9170	0.9075
0.9894	0.9852	0.9808	0.9778	0.9755	0.9719	0.9698	0.9673	0.9652	0.9630
0.9850	0.9764	0.9676	0.9600	0.9528	0.9446	0.9380	0.9310	0.9244	0.9164
0.9887	0.9840	0.9791	0.9756	0.9732	0.9691	0.9669	0.9646	0.9621	0.9595

**Table 4: PSNR Values of each column corresponds to the noise values from (0.01, 0.02 ....0.1)**

20.0556	17.2037	15.5640	14.4672	13.6488	12.9794	12.4607	12.0382	11.6684	11.3334
28.1933	26.0360	24.6041	23.6033	22.8452	22.2084	21.6541	21.2137	20.8403	20.4559
30.0752	28.6189	27.3919	26.6947	26.0765	25.4371	25.1154	24.7155	24.2687	23.8281
29.0194	27.3475	26.0987	25.1874	24.5357	23.8283	23.3585	22.8704	22.5105	22.0569
31.2812	29.8213	28.6591	27.9049	27.3660	26.6331	26.2181	25.7419	25.2827	24.8163
29.7848	27.8495	26.4843	25.5910	24.8782	24.2007	23.7202	23.2646	22.8722	22.4394
31.0144	29.4646	28.2444	27.4584	26.9158	26.1631	25.7526	25.3019	24.8368	24.3628

**GRAPHICAL REPRESENTATION OF PARAMETERS**

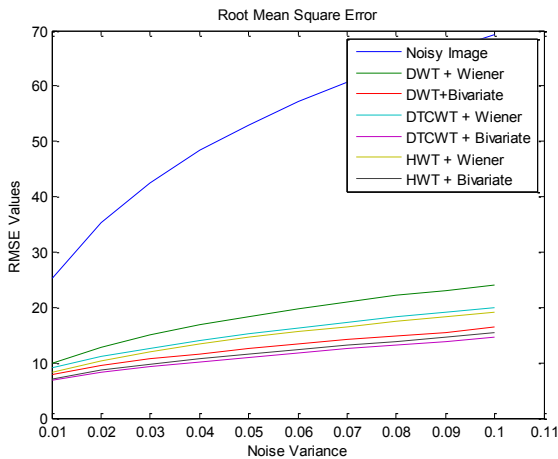


**Figure 14: RMSE Comparison**

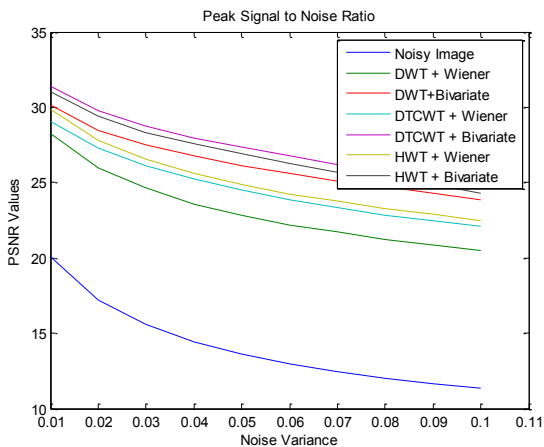


**Figure 15: PSNR Comparison**

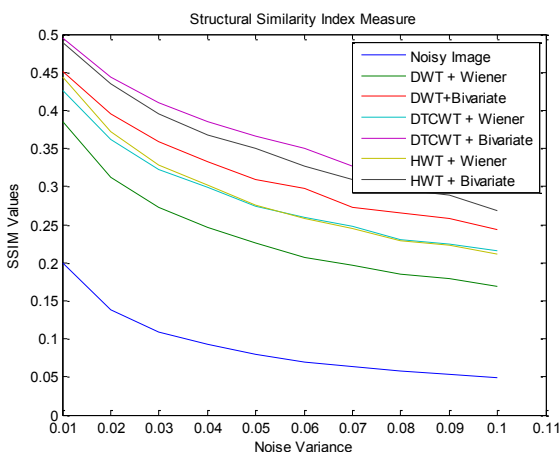


**Figure 16: SSIM Comparison**

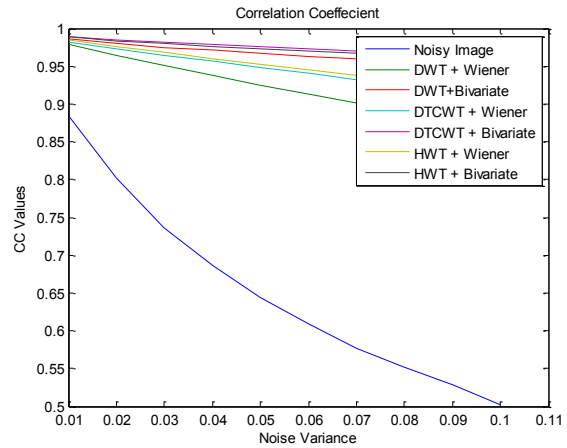


**Figure 17: Correlation Coefficient Comparison**

**CONCLUSION**

The de-noising of image is initial step in image processing. The quality of the de-noised image depends on the two major parts: wavelet transform for decomposition of image and adaptive wiener filtering in wavelet domain and spatial domain. The performance of the local adaptive wavelet image de-noising method is good compared to modified de-noising method in terms of PSNR between de-noised image and original image. But the edges of the image are smoothed such that the clarity of the image gets damaged. So, in order to overcome this drawback we conclude that bivariate shrink technique is more effective for suppression of noisy compared to local adaptive wiener filter. Thus the image after de-noising have a better visual effect and preserve the detail edges of image.

**REFERENCES**

- 1] Parmar, Jignasa M., and S. A. Patil. "Performance evaluation and comparison of modified denoising method and the local adaptive wavelet image denoising method." *Intelligent Systems and Signal Processing (ISSP), 2013 International Conference on*. IEEE, 2013.
- 2] Song, Qingkun, et al. "Image Denoising Based on Mean Filter and Wavelet Transform." *Advanced Information Technology and Sensor Application (AITS), 2015 4th International Conference on*. IEEE, 2015.
- 3] Hussain, Israr, and Hujun Yin. "A novel wavelet thresholding method for adaptive image denoising." *Communications, Control and Signal Processing, 2008. ISCCSP 2008. 3rd International Symposium on*. IEEE, 2008.
- 4] Sazonov, V.V., Shcherbakov, M.A. and Vasilyev, V.A., 2015, October. Modified Wiener filter. In *Biomedical Engineering and Computational Technologies (SIBIRCON), 2015 International Conference on* (pp. 193-196). IEEE.
- 5] Firoiu, Ioana, et al. "Image denoising using a new implementation of the hyperanalytic wavelet transform." *IEEE Transactions on Instrumentation and Measurement* 58.8 (2009): 2410-2416.

- 6] Zhang, Huipin, Aria Nosratinia, and R. O. Wells. "Image denoising via wavelet-domain spatially adaptive FIR Wiener filtering." *Acoustics, Speech, and Signal Processing, 2000. ICASSP'00. Proceedings. 2000 IEEE International Conference on*. Vol. 4. IEEE, 2000.
- 7] Kazubek, Marian. "Wavelet domain image denoising by thresholding and Wiener filtering." *IEEE Signal Processing Letters* 10.11 (2003): 324-326.
- 8] Mohideen, S. Kother, S. Arumuga Perumal, and M. Mohamed Sathik. "Image de-noising using discrete wavelet transform." *International Journal of Computer Science and Network Security* 8.1 (2008): 213-216.
- 9] Ke, Li, Weiqi Yuan, and Yang Xiao. "An improved wiener filtering method in wavelet domain." *Audio, Language and Image Processing, 2008. ICALIP 2008. International Conference on*. IEEE, 2008.
- 10] Nafornta, C., & Isar, A. (2012, November). A complete second order statistical analysis of the Hyperanalytic Wavelet Transform. In *Electronics and Telecommunications (ISETC), 2012 10th International Symposium on* (pp. 227-230). IEEE.
- 11] Firoiu, I. Complex Wavelet Transform. Application to Denoising. Diss. *PhD thesis*, Universitatea Politehnica, Timisoara, 2010.